TÜBİTAK

Turkish Journal of Physics

http://journals.tubitak.gov.tr/physics/

Research Article

Turk J Phys
(2018) 42: 136 – 145
© TÜBİTAK
doi:10.3906/fiz-1706-6

The influence of deposit composition controlled by changing the relative Fe ion concentration on properties of electroplated nanocrystalline Co-Fe-Cu ternary thin films

Umut SARAÇ[1,*], Malik KAYA[2], M. Celalettin BAYKUL[3]
[1]Department of Science Education, Faculty of Education, Bartın University, Bartın, Turkey
[2]Vocational School of Health Services, Eskişehir Osmangazi University, Eskişehir, Turkey
[3]Department of Metallurgical and Materials Engineering, Department of Engineering, Eskişehir Osmangazi University, Eskişehir, Turkey

Received: 05.06.2017 • **Accepted/Published Online:** 20.12.2017 • **Final Version:** 26.04.2018

Abstract: Ternary Co-Fe-Cu thin films with 78.5–92.4 at.% Co, 4.1–17.9 at.% Fe, and 3.1–3.6 at.% Cu were electroplated at ambient temperature from electrolytes with different relative Fe ion concentrations with respect to the Co ion concentration on the glass substrates coated with indium tin oxide (ITO). It was revealed that the Fe is more easily deposited than Co for all electrolyte conditions. The phase structure of the films changed from a mixture of hcp Co and fcc/hcp Co to a mixture of fcc/hcp Co and bcc Fe and the mean crystallite size diminished with increasing Fe content within the deposits. A shift in the peak position of the fcc/hcp Co phase towards lower 2θ angles with increasing Fe content within the deposits was observed and the reason for that was discussed. There was also a transition in the surface morphological structure of the films from an acicular-like type structure to a cauliflower-like type structure. The changes that appeared in the surface morphology were related to phase structure, which was affected considerably by the deposit composition.

Key words: Electrochemical deposition technique, Co-Fe-Cu ternary thin films, phase structure, SEM analyses, deposit composition, anomalous codeposition

1. Introduction

Thin films of Fe, Co, and Ni and their alloys prepared using electrochemical deposition techniques have gained considerable interest owing to their potential applications in micro electromechanical system devices and data storage media [1–3]. Soft deposits based on Co-Fe are important materials and it has been reported that the addition of one or more elements including Ni and Cu into Co-Fe magnetic thin films can help to improve their specific properties [4–6]. However, few studies have been focused on ternary Co-Fe-Cu magnetic thin film systems electrochemically deposited under different experimental conditions. In an earlier work [7], the effect of the pulse parameter on ternary Co-Fe-Cu deposits with the Cu content varying between 5 wt.% and 20 wt.% was reported. Kalu et al. studied the corrosion characteristics of Co-Fe-Cu films with and without phosphorus [6]. Mehrizi et al. investigated the properties of Co-Fe-Cu deposits electrochemically deposited at various applied current densities [4]. In that study, the Co-Fe-Cu films containing up to 10 at.% of Cu content were observed to have optimum required properties [4]. In another study [8], the microstructural and magnetic

*Correspondence: usarac428@hotmail.com

properties of Co-Fe-Cu films were studied according to Fe ion concentration within the electrolyte solution. On the other hand, Co-Fe-Cu magnetic films were electrochemically fabricated at different deposition cathode potentials [9] and from electrolytes with natural pH values and containing different sodium citrate dosages [10]. As a result, these studies revealed that the experimental conditions have an important effect on the features of electrochemically deposited ternary Co-Fe-Cu films. The less noble metal is deposited preferentially compared to the more noble metal for a wide range of electroplating conditions in the electrochemical deposition of the films with iron-group metals, reflecting the formation of anomalous codeposition [11]. Furthermore, chemical composition of the electrochemically deposited magnetic metallic thin films is also well known to be affected directly by the relative concentration of metals used in the electrolyte solution [8,12–15].

In this research, the influence of the deposit composition of Co-Fe-Cu ternary thin films on the characterized properties was reported. The results revealed that the morphological structure and the microstructural properties of the films grown onto indium tin oxide (ITO) substrates were significantly influenced by the deposit composition, which was affected by the relative Fe ion concentration of aqueous solution with respect to Co ion concentration.

2. Materials and methods

The fabrication of ternary Co-Fe-Cu magnetic thin films was performed using an electrochemical deposition technique. The films were deposited from an electrolyte solution containing Co sulfate, Fe sulfate, Cu sulfate, and boric acid. All of the experiments were performed at ambient conditions (temperature and pressure) without stirring. The electrolyte solutions were freshly prepared with deionized water and chemicals for each deposition of films. The temperature of the prepared electrolyte solution was 25 ± 1 °C and the pH value was 4.2 ± 0.1. The Cu ion concentration was 0.001 M and the boric acid concentration was 0.2 M in all electrolyte solutions. In order to obtain electrolyte solutions with different relative Fe ion concentrations with respect to Co ion concentration, the Fe ion concentration of the bath was increased from 0.005 M to 0.025 M, while the Co ion concentration was decreased from 0.195 to 0.175 M. However, in all experiments, the total concentration of Fe and Co ions was 0.2 M. In this study, the electrolyte solutions were characterized by the relative Fe ion concentration $c_{(ion,Fe)}$ within the electrolyte solutions. The relative Fe ion concentrations $c_{(ion,Fe)} = [FeSO_4]/[FeSO_4 + CoSO_4] \times 100$ [16] within the electrolytes with respect to Co ion concentration were 2.5%, 5.0%, and 12.5%.

The electrochemical deposition processes were performed in a conventional three-electrode cell composed of working, counter, and reference electrodes. In the experiments, a potentiostat/galvanostat (VersaSTAT 3) with computer control was used. Glass substrates coated with ITO (sheet-resistance of about 8–12 Ω/sq.) were used as the working electrode. Prior to starting the electrochemical deposition of the films, the substrate surfaces were cleaned in medium containing acetone for 5 min and ethanol for 5 min, respectively. Finally, they were ultrasonically rinsed with deionized water for 10 min using an ultrasonic bath. The counter electrode was a platinum wire. The reference electrode was a saturated calomel electrode. In all experiments, the electrochemical deposition process was performed at a constant current density of –12 mA/cm^2 and the thicknesses of the films were designed as $\sim$0.5 μm by controlling the deposition time based on Faraday's law.

The identification of the microstructural properties of the Co-Fe-Cu ternary thin films depending on the Fe content was carried out using X-ray diffraction (XRD; Rigaku SmartLab) with CuKα radiation ($\lambda = 0.154059$ nm) in the range of 40° to 49° with 0.01° steps. The deposit morphologies were revealed by means of scanning electron microscopy (SEM; Zeiss Supra 40Vp). Energy dispersive X-ray (EDX) spectroscopy was utilized for the

determination of the chemical composition according to the relative Fe ion concentration within the electrolyte and metal proportions in all obtained thin films were given in atomic percentages (at.%) in the whole text. The growth characteristics of the films electroplated at various relative Fe ion concentrations within the electrolyte solution were followed by means of galvanostatic potential-time transient curves, which were recorded during the electroplating process.

3. Results and discussion

In this research, we have investigated the influence of the deposit composition on the characterized features of Co-Fe-Cu ternary magnetic thin films electrochemically synthesized onto ITO-coated glass substrates. In order to obtain films with different compositions, the films were electrochemically deposited from electrolytes with different relative Fe ion concentrations with respect to Co ion concentration using the procedure mentioned in Section 2. As a first step of this research, the growth characteristics of the films were determined by means of galvanostatic potential-time transient curves. The curves with respect to relative Fe ion concentration $c_{(ion,Fe)}$ within the electrolyte are shown in Figure 1. Figure 1 reveals that Co-Fe-Cu ternary magnetic thin films can be grown uniformly onto ITO substrates since the cathode potential remains almost stable during electrochemical deposition of the films regardless of the relative Fe ion concentration $c_{(ion,Fe)}$ within the electrolyte. Additionally, the cathode potential slightly increases when the relative Fe ion concentration $c_{(ion,Fe)}$ within the electrolyte increases. Similar findings were also revealed in a study carried out under different experimental conditions [8].

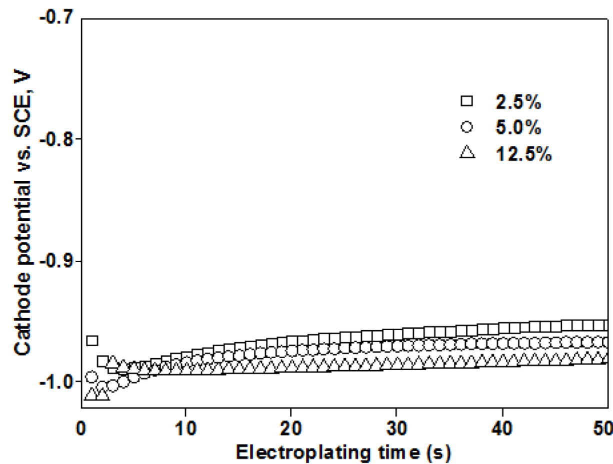

Figure 1. Galvanostatic potential–time transient curves of the electrochemically deposited ternary Co-Fe-Cu thin films as a function of relative Fe ion concentration $c_{(ion,Fe)}$ within the electrolyte.

The compositional analyses carried out using EDX revealed that the Co-Fe-Cu film deposited from an electrolyte with $c_{(ion,Fe)}$ = 2.5% consists of 92.4 at.% Co, 4.1 at.% Fe, and 3.5 at.% Cu. The film electrochemically fabricated from an electrolyte with $c_{(ion,Fe)}$ = 5.0% has 89.1 at.% Co, 7.8 at.% Fe, and 3.1 at.% Cu while the film grown from an electrolyte with $c_{(ion,Fe)}$ = 12.5% contains 78.5 at.% Co, 17.9 at.% Fe, and 3.6 at.% Cu. These results reveal that the Fe content within the deposits increases and the Co content decreases with the increase of the relative Fe ion concentration $c_{(ion,Fe)}$ within the electrolyte. The Cu content within the films is found to be fairly constant and low. The relative Fe content z_{Fe} = [Fe]/[Fe + Co] × 100

within the films with respect to Co content is determined [16] and the variation of z_{Fe} within the deposits as a function of $c_{(ion,Fe)}$ within the electrolyte solution is given in Figure 2. The z_{Fe} values within the deposits are found to be always higher than $c_{(ion,Fe)}$ values within the electrolyte solution. These findings reflect that the less noble Fe is always preferentially deposited compared to the more noble Co, revealing the formation of the anomalous codeposition behavior regardless of the $c_{(ion,Fe)}$ within the electrolyte solution. The anomalous codeposition behavior of Co-Fe was also revealed in electrochemically deposited Co-Fe [15], Co-Fe-Cu [17], and Co-Fe/Cu [16], supporting our results. The anomalous codeposition behavior was ascribed to the formation of iron hydroxide ions on the cathode surface in earlier studies [15,17,18]. Furthermore, a change in the degree of anomalous codeposition behavior as a function of $c_{(ion,Fe)}$ within the electrolyte is also investigated. For this purpose, the selective ratio of Fe-Co, Co-Cu, and Fe-Cu is determined as a function of relative Fe ion concentration $c_{(ion,Fe)}$ within the electrolyte. For example, the selective ratio of Co-Ni is described as the ratio of Co/Ni within the film to the ratio of $CoSO_4/NiSO_4$ within the electrolyte solution [19]. The obtained values of the selective ratio of Fe-Co, Co-Cu, and Fe-Cu as a function of $c_{(ion,Fe)}$ are shown in Figure 3. From Figure 3, it may be concluded that an increment in the relative Fe ion concentration $c_{(ion,Fe)}$ within the electrolyte leads to a slight decrement in the degree of anomalous codeposition behavior of Co-Fe. The values of the selective ratio are lower than 1 for Fe-Cu and Co-Cu irrespective of relative Fe ion concentration $c_{(ion,Fe)}$ in the electrolyte, reflecting that more noble copper is always preferentially deposited compared to less noble Co and Fe. Thus, it may be concluded that the codeposition behaviors of Fe-Cu and Co-Cu are normal in the electrochemical deposition process of Co-Fe-Cu.

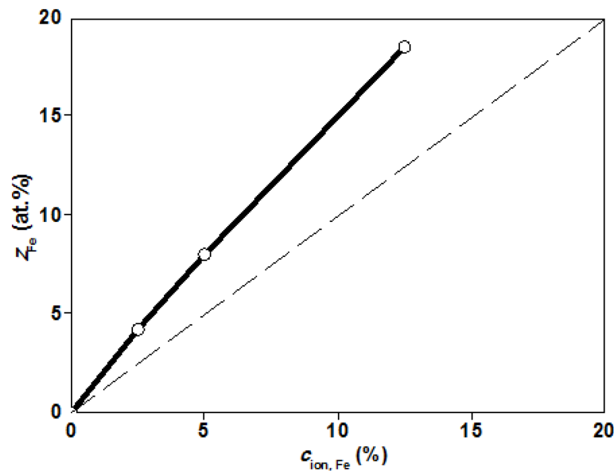

Figure 2. The variation of relative Fe content z_{Fe} of the deposits with respect to relative Fe ion concentration $c_{(ion,Fe)}$ of the electrolytes. The dashed line with a slope equal to 1 represents the conditions of equilibrium codeposition.

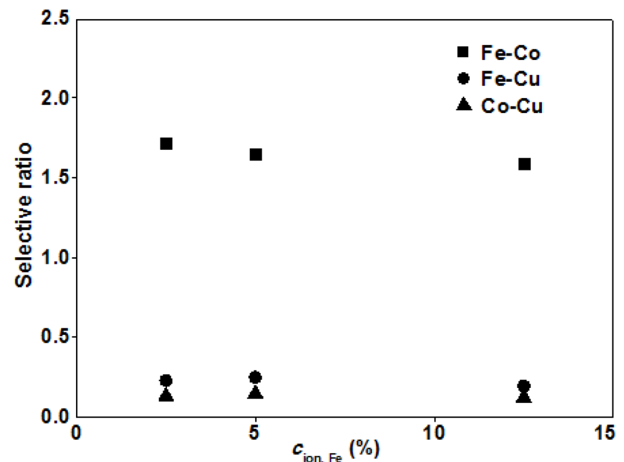

Figure 3. Dependence of the selective ratio of Fe-Co, Fe-Cu, and Co-Cu on the relative Fe ion concentration $c_{(ion,Fe)}$ in the electrolyte solution.

The crystal structure of the electrochemically deposited Co-Fe-Cu ternary thin films was analyzed using XRD according to the deposition composition. The results of the XRD analyses are indicated in Figure 4. The XRD patterns reveal that the phase structure of the Co-Fe-Cu ternary deposits is significantly influenced by the deposit composition. In previous studies, it was reported that the fcc Co (111) line strongly coincides with the hcp Co (002) line [20,21]. Therefore, it is difficult to distinguish orientated hcp (002) or fcc Co (111). As

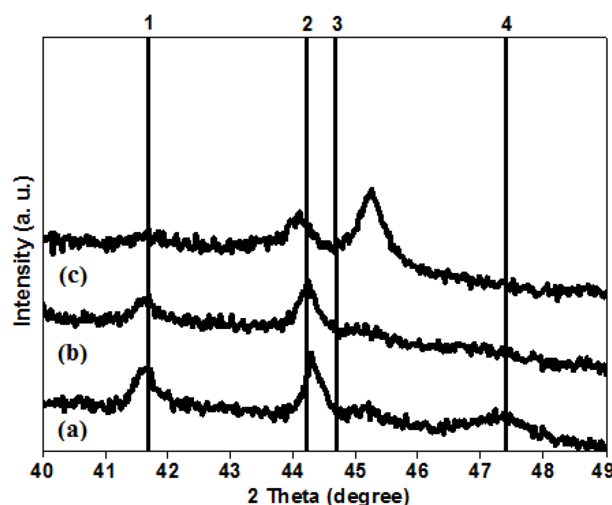

Figure 4. XRD patterns of the electrochemically deposited thin films of ternary Co-Fe-Cu with different compositions: a) 92.4 at.% Co, 4.1 at.% Fe, 3.5 at.% Cu; b) 89.1 at.% Co, 7.8 at.% Fe, 3.1 at.% Cu; and c) 78.5 at.% Co, 17.9 at.% Fe, 3.6 at.% Cu. The vertical solid lines show the pure metal line positions (100) hcp Co (*1), (111) fcc Co and (002) hcp Co (*2), (110) bcc Fe (*3), and (101) hcp Co (*4). The pure metal line positions were obtained from Refs. [9,20,21].

seen from Figure 4a, the diffraction peaks of hcp Co (100), hcp Co (101), and fcc Co (111)/hcp Co (002) are observed for the film with low Fe content of 4.1 at.% and high Co content of 92.4 at.%. The film contains hcp (100) and fcc Co (111)/hcp Co (002) diffraction peaks and the hcp Co (101) peak disappears at intermediate Fe content of 7.8 at.% (Figure 4b). The film with high Fe content of 17.9 at.% and low Co content of 78.5 at.% has fcc Co (111)/hcp Co (002) and bcc Fe (110) diffraction peaks without hcp Co (100) and hcp Co (101) peaks (Figure 4c). Furthermore, the intensity of the fcc Co (111)/hcp Co (002) peak decreases with increasing Fe content within the films. This change observed in the fcc Co (111)/hcp Co (002) peak intensity may be ascribed to a decrease in the Co content of the films. On the other hand, the absence of fcc Cu peaks in all XRD patterns can probably be attributed to the low Cu content within the films (about 3 at.%). In a previous study, the reflection from the fcc Cu diffraction peak was not observed when the Cu content was lower than 15 at.% [4]. Additionally, there is no reflection from the diffraction peak of the bcc phase structure of Fe in the XRD patterns of the deposits with low Fe contents of 4.1 at.% and 7.8 at.%, as can be seen from Figures 4a and 4b, respectively. Similarly, no reflection from the diffraction peak of the bcc phase structure of Fe was observed in previous studies carried out with electrochemically deposited Co-Fe-Cu ternary films when the Fe content within the films was lower than 11 at.% [4] and 14 at.% [8]. As a result, we reveal that the phase structure changes from a mixture of hcp Co and fcc/hcp Co to a mixture of fcc/hcp Co and bcc Fe with increasing Fe content within the films, as also summarized in Table 1. However, it must be mentioned here that there are some microstructural differences between the XRD patterns of the present study and earlier studies. For example, the study showed that the phase structure changes from a mixture of fcc Cu and fcc Co to single fcc Co and then to a mixture of fcc Co and bcc Fe with the increase of applied current density due to the change of film composition [4]. In another study, the phase structure of the films was revealed to change from a mixture of fcc and hcp to single fcc and then to single bcc with increasing Fe content within the films affected considerably by the amount of Fe ions within the bath [8]. These microstructural differences may occur due to the different electroplating variables used in the experiments, such as substrate type, electrolyte concentration, or additives.

The microstructural properties of the electrochemically deposited films are well known to be affected strongly by these electroplating variables.

Table 1. Evolution of phase structure, lattice spacing, and mean crystallite size of the electrochemically deposited ternary Co-Fe-Cu thin films with respect to deposit composition.

Deposit composition			Phase structure	Lattice spacing		Crystallite size
Co (at.%)	Fe (at.%)	Cu (at.%)	(XRD)	fcc/hcp Co (nm)	bcc Fe (nm)	(nm)
92.4	4.1	3.5	hcp and fcc/hcp	$0.20413 \pm 8 \times 10^{-5}$	-	29 ± 4
89.1	7.8	3.1	hcp and fcc/hcp	$0.20456 \pm 5 \times 10^{-5}$	-	27 ± 3
78.5	17.9	3.6	fcc/hcp and bcc	$0.20523 \pm 5 \times 10^{-5}$	$0.2004 \pm 6 \times 10^{-5}$	21 ± 3

The mean crystallite sizes were calculated using the Scherrer formula [22]. For this purpose, the full-width at half maximum values of more prominent fcc Co (111) and bcc Fe (110) diffraction peaks were used. The films exhibit nanocrystalline structures regardless of deposit composition since the mean sizes of crystallites are found to be in the range between 21 and 29 nm. It is also revealed that the mean size of the crystallites decreases with increasing Fe content of the films achieved by increasing the relative Fe ion concentration within the bath (see Table 1). In our present study, the smallest crystallite size obtained for the film with high Fe content of 17.9 at.% may be due to the formation of the bcc Fe phase as well as the fcc/hcp Co phase, as can be seen from Figure 4c [4]. On the other hand, as can be seen from Figure 1, an increase in the cathode potential with increasing relative Fe ion concentration may also lead to a decrement in the mean size of the crystallites. It was reported in previous studies that the mean size of the crystallites decreases with increasing cathode potential (or applied current density) in electrochemically deposited Fe-Cu [23], Co-Cu [24, 25], and Co-Fe-Cu films [4].

On the other hand, the interplanar spacings of the fcc Co (111)/hcp Co (002) phase are found to be 0.20413, 0.20456, and 0.20523 nm for the Co-Fe-Cu ternary thin films containing 4.1, 7.8, and 17.9 at.% Fe, respectively (see Table 1). An increase in the interplanar spacing of the fcc Co (111)/hcp Co (002) phase gives rise to a shift of the central intensity maximum of the fcc Co (111)/hcp Co (002) diffraction peak towards lower 2θ angles with increasing Fe content within the films, as can be seen from the XRD patterns. The interplanar spacings of the fcc Co (111)/hcp Co (002) phase for the films with 4.1 and 7.8 at.% Fe are determined to be smaller than that of the pure fcc Co (111) phase (0.20465 nm) [20,21], while the interplanar spacing for the film with 17.9 at.% Fe is higher compared to the interplanar spacing of the pure fcc Co (111) phase. On the other hand, the interplanar spacings of the fcc Co (111)/hcp Co (002) phase are found to be higher than that of the pure hcp Co (002) phase (0.20303 nm) irrespective of the Fe content of the deposits [20,21]. An increase in the interplanar spacing of the fcc Co (111)/hcp Co (002) phase with increasing Fe content within the deposit structure may be due to the alloying of more and more Fe to the Co phase. An incorporation of Fe atoms into the fcc Co (111)/hcp Co (002) phase may result in an increase in the interplanar spacing of the fcc Co (111)/hcp Co (002) phase since the atomic radius is larger for Fe (0.172 nm) than Co (0.167 nm) [26,27]. On the other hand, as seen from Table 1, the interplanar spacing of the bcc Fe (110) phase is found to be about 0.2004 nm, which is smaller than that of the pure bcc Fe (110) phase (0.2027 nm) [9]. Thus, it may be suggested that an incorporation of smaller Co atoms into the bcc Fe (110) phase leads to a decrement in the interplanar spacing of the bcc Fe (110) phase, as also observed in electrochemically fabricated Fe-Co-Ni magnetic films [26,27].

Another possible reason for a change in the interplanar spacing with increasing Fe content within the deposits is the lattice strain, since it is related to the distortion of the crystal lattice [20,21]. In order to calculate

the lattice strain (ε) in the fcc Co (111)/hcp Co (002) and bcc Fe (110) phases of the deposits, a well-known equation was used [20,21]:

$\varepsilon = (d_{deposit} - d_{pure})/d_{pure}$, where $d_{deposit}$ is the interplanar spacing in the deposit and d_{pure} is the interplanar spacing in the pure metal, respectively. The estimated lattice strains as a function of Fe content within the deposits are shown in Table 2. The lattice strain in the fcc Co (111)/hcp Co (002) phase is determined to be negative for the films with 4.1 and 7.8 at.% Fe and positive for the film with 17.9 at.% Fe if the fcc Co (111)/hcp Co (002) phase is related to fcc Co (111). The negative (positive) lattice deformation represents the formation of tensile (compressive) type residual stress [20,21]. Hence, it may be concluded that the fcc Co (111)/hcp Co (002) phase of the films including 4.1 and 7.8 at.% Fe is under a tensile type residual stress while the fcc Co (111)/hcp Co (002) phase in the Co-Fe-Cu ternary thin film with 17.9 at.% Fe is under a compressive type residual stress. On the other hand, the nature of the residual stress in the fcc Co (111)/hcp Co (002) phase is found be compressive for all films if the fcc Co (111)/hcp Co (002) phase is related to hcp Co (002). From Table 2, it is easily concluded that the fcc Co (111)/hcp Co (002) phase in the Co-Fe-Cu ternary thin film with 17.9 at.% Fe is under a compressive type residual stress regardless of the reference Co phase, i.e. fcc Co (111) or hcp Co (002). As to the bcc Fe (110) phase, the lattice strain is determined to be negative for the film with 17.9 at.% Fe, indicating the formation of tensile type residual stress due to the negative lattice deformation.

Table 2. Evolution of lattice strain and surface morphology of the electrochemically fabricated ternary Co-Fe-Cu thin films as a function of Fe content within the deposits. The relative errors of ε [(fcc Co (111)] and ε [(hcp Co (002)] estimated from the relative errors of the interplanar spacings in the deposits given in Table 1 are 0.42×10^{-3}, 0.25×10^{-3}, and 0.24×10^{-3} for the deposits with 4.1, 7.8 and 17.9 at.% Fe, respectively. The relative error of ε [(bcc Fe (110)] is 0.29×10^{-3}.

Fe content (at.%)	ε [(fcc Co (111)]	ε [(hcp Co (002)]	ε [(bcc Fe (110)]	Morphology (SEM)
4.1	-2.54×10^{-3}	5.42×10^{-3}	-	Acicular-like
7.8	-0.44×10^{-3}	7.54×10^{-3}	-	Acicular-like
17.9	2.83×10^{-3}	10.84×10^{-3}	-11.35×10^{-3}	Cauliflower-like

The surface morphological structure was studied with respect to deposit composition using a SEM technique. The SEM micrographs with 30,000× magnification are indicated in Figure 5. It is clearly seen that there are no cracks on the film surfaces and thin films of ternary Co-Fe-Cu can cover the ITO substrates well. As seen from Figures 5a and 5b, the produced films with Fe contents of 4.1 at.% and 7.8 at.% exhibit a morphology consisting of acicular-like type structures. If the findings regarding the surface morphological structure revealed in previous studies are considered [8,9], the acicular-like type structure observed in the present study may be attributed to higher Co contents of 89.1 at.% and 92.4 at.% within the films. On the other hand, the electrochemically fabricated film with high Fe content of 17.9 at.% and low Co content of 78.5 at.% has a morphology with cauliflower-like type structures (Figure 5c). Additionally, the agglomeration of structures on the film surfaces is observed, resulting in clustering. However, the surface morphology shows a more compact feature with smaller clusters at higher Fe contents. The rate of nucleation may increase with increasing Fe content and therefore the film exhibits a more compact structure at higher Fe contents. Consequently, a transition in the surface morphology of the films from acicular-like type structure to cauliflower-like type structure with increasing Fe content within the deposit is clearly evident from the SEM micrographs, as also listed in Table 2. This transition occurring in the surface morphology of the films with increasing Fe

content may be attributed to changes observed in the phase structure. It is easily concluded from Figures 4 and 5 (XRD patterns and SEM micrographs, respectively) that the films with a mixture of hcp Co and fcc/hcp Co phase structure have a morphology with acicular-like type structures, whereas the film with a mixture of fcc/hcp Co and bcc Fe phase structure exhibits a cauliflower-like type morphology.

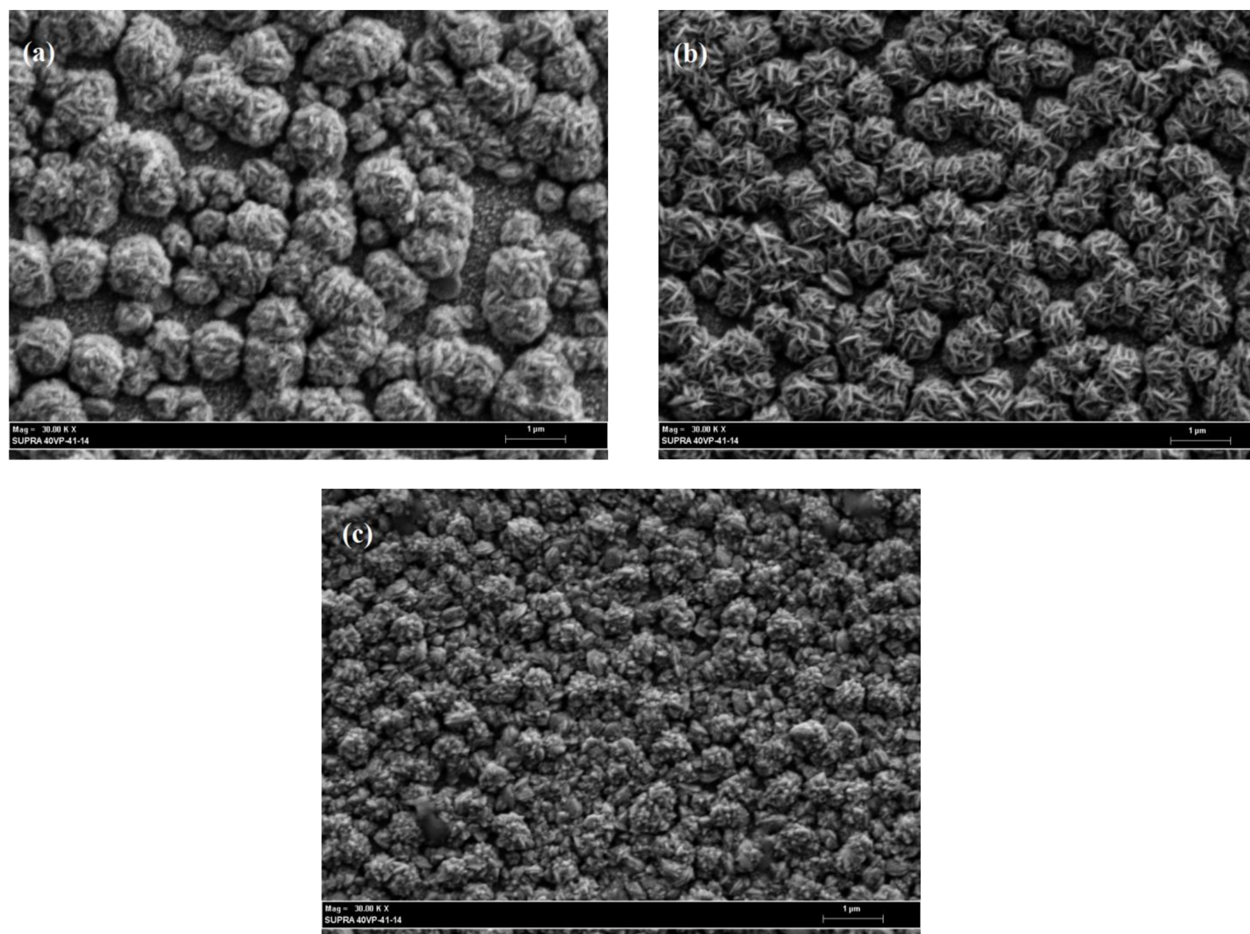

Figure 5. SEM micrographs of the electrochemically deposited ternary Co-Fe-Cu thin films with different compositions: a) 92.4 at.% Co, 4.1 at.% Fe, 3.5 at.% Cu; b) 89.1 at.% Co, 7.8 at.% Fe, 3.1 at.% Cu; and c) 78.5 at.% Co, 17.9 at.% Fe, 3.6 at.% Cu.

4. Conclusions

In this research, thin films of ternary Co-Fe-Cu with different compositions were fabricated from electrolyte solutions with various relative Fe ion concentrations with respect to Co ion concentration onto ITO substrates using an electrochemical deposition technique. The main purpose of this work was to investigate the relationship between microstructures and morphological features according to deposit composition. EDX analyses showed that the films consisted of 78.5–92.4 at.% Co, 4.1–17.9 at.% Fe, and 3.1–3.6 at.% Cu. It was found that the codeposition of Co-Fe was anomalous but Fe-Cu and Co-Cu exhibited normal codeposition behavior in electrochemical deposition of Co-Fe-Cu irrespective of the relative Fe ion concentration within the electrolytes. It was also revealed that an enhancement in the relative Fe ion concentration of the electrolyte gave rise to a

slight decrement in the degree of anomalous codeposition. The phase structure changed from a mixture of hcp Co and fcc/hcp Co to a mixture of fcc/hcp Co and bcc Fe and the mean crystallite size decreased with increasing Fe content within the films. There was a shift in the peak position of the fcc/hcp Co phase towards lower 2θ angles with increasing Fe content within the deposits. This shift was attributed to the alloying of more and more Fe to the Co phase and/or the distortion of the crystal lattice due to the lattice strain. The surface morphology of the Co-Fe-Cu ternary deposits also changed from an acicular-like type structure to a cauliflower-like type structure with increasing Fe content and exhibited a more compact feature at high Fe content. Accordingly, this study revealed that the Co-Fe-Cu ternary thin films exhibit a mixture of hcp Co and fcc/hcp Co phase structures, higher crystallite sizes, and an acicular-like type morphology at low Fe contents while the film displays a mixture of fcc/hcp Co and bcc Fe phase structures, lower crystallite sizes, and cauliflower-like type morphology with more compact feature at high Fe content.

Acknowledgment

This work was financially supported by the Scientific Research Projects Commission of Bartın University under project number 2013.2.98.

References

[1] Myung, N. V.; Nobe, K. *J. Electrochem. Soc.* **2001**, *148*, C136-C144.

[2] Myung, N. V.; Park, D. Y.; Yoo, B. Y.; Sumodjo, P. T. A. *J. Magn. Magn. Mater.* **2003**, *265*, 189-198.

[3] Kim, D.; Park, D. Y.; Yoo, B. Y.; Sumodjo, P. T. A.; Myung, N. V. *Electrochim. Acta* **2003**, *48*, 819-830.

[4] Mehrizi, S.; Sohi, M. H.; Shafahian, E.; Khangholi, A. A. *J. Mater. Sci. Mater. Electron.* **2012**, *23*, 1174-1181.

[5] Mehrizi, S.; Sohi, M. H.; Ebrahimi, S. A. S. *Surf. Coat. Technol.* **2011**, *205*, 4757-4763.

[6] Kalu, E. E.; Bell, R.; Dupree, M. *Mater. Chem. Phys.* **2010**, *124*, 689-693.

[7] Bradley, P. E.; Janossy, B.; Landolt, D. *J. Appl. Electrochem.* **2001**, *31*, 137-144.

[8] Kockar, H; Ozergin, E.; Karaagac, O.; Alper, M. *J. Alloys Compd.* **2014**, *586*, S326-S330.

[9] Kockar, H; Ozergin, E.; Karaagac, O.; Alper, M. *J. Mater. Sci. Mater. Electron.* **2013**, *24*, 2562-2567.

[10] Mehrizi, S.; Sohi, M. H. *J. Supercond. Nov. Magn.* **2014**, *27*, 1701-1708.

[11] Brenner, A. *Electrodeposition of Alloys Principles and Practice*; Academic Press: New York, NY, USA, 1963.

[12] Sarac, U.; Baykul, M. C. *Adv. Mater. Sci. Eng.* **2013**, *2013*, 1-7.

[13] Sarac, U.; Baykul, M. C. *J. Mater. Sci. Mater. Electron.* **2014**, *25*, 2554-2560.

[14] Sarac, U.; Baykul, M. C.; Uguz, Y. *J. Supercond. Nov. Magn.* **2015**, *28*, 3105-3110.

[15] Qiang, C.; Xu, J.; Xiao, S.; Jiao, Y.; Zhang, Z.; Liu, Y.; Tian, L.; Zhou, Z. *Appl. Surf. Sci.* **2010**, *257*, 1371-1376.

[16] Tóth, B. G.; Péter, L.; Pogány, L.; Révész, Á.; Bakonyi, I. *J. Electrochem. Soc.* **2014**, *161*, D154-D162.

[17] Ramazani, A.; Almasi-Kashi, M.; Golafshan, E.; Arefpour, M. *J. Cryst. Growth* **2014**, *402*, 42-47.

[18] Atalay, F. E.; Kaya, H.; Atalay, S.; Tari, S. *J. Alloys Compd.* **2009**, *469*, 458-463.

[19] Phan, N. H.; Schwartz, M.; Nobe, K. *J. Appl. Electrochem.* **1991**, *21*, 672-677.

[20] Rafaja, D.; Schimpf, C.; Klemm, V.; Schreiber, G.; Bakonyi, I.; Péter, L. *Acta Mater.* **2009**, *57*, 3211-3222.

[21] Rafaja, D.; Schimpf, C.; Schucknecht, T.; Klemm, V.; Péter, L.; Bakonyi, I. *Acta Mater.* **2011**, *59*, 2992-3001.

[22] Wilson, A. J. C. *Proc. Phys. Soc. Lond.* **1962**, *80*, 286-294.

[23] Sarac, U.; Baykul, M. C. *J. Mater. Sci. Technol.* **2012**, *28*, 1004-1009.

[24] Sarac, U.; Baykul, M. C. *J. Mater. Sci. Mater. Electron.* **2014**, *25*, 39-45.

[25] Min, J. H.; Wu, J. H.; Cho, J. U.; Liu, Q. X.; Lee, J. H.; Ko, Y. D.; Chung, J. S.; Lee, J. H.; Kim, Y. K. *J. Magn. Magn. Mater.* **2006**, *304*, e100-e102.

[26] Nam, H. S.; Yokoshima, T.; Nakanishi, T.; Osaka, T.; Yamazaki, Y.; Lee, D. N. *Thin Solid Films* **2001**, *384*, 288-293.

[27] Liu, X.; Zangari, G.; Shamsuzzoha, M. *J. Electrochem. Soc.* **2003**, *150*, C159-C168.